Research Article

# Experimental Study and Analysis of Fretting Wear and its Influence on Functionality of Mechanical Components

Jyothilakshmi Ramaswamy, Nandeesha Hosanagara Lokesha* and Deepak Swamy
Department of Mechanical Engineering, M S Ramaiah Institute of Technology, Bengaluru, Karnataka, India

* Corresponding author. E-mail: hl.nandeesha@gmail.com DOI: 10.14416/j.asep.2023.03.005
Received: 15 October 2022; Revised: 10 December 2022; Accepted: 13 March 2023; Published online: 28 March 2023


**Abstract**
Fretting occurs when there is tangentially low-amplitude vibrational motion (range tens of nanometres to tens of micrometers) between nominally stationary contact surfaces. This is a common occurrence as most machines are exposed to vibration both in transit and in operation. Contacts that appear to have no relative movement, such as press-fit, can actually slide on a scale of 1 μm with alternating pendulum loads. It is very difficult to eliminate such movements and the resulting friction. Fretting wear and frictional fatigue occur on almost every machine and otherwise cause a total failure of robust components. Studies have shown that, in contrast to other forms of wear, the frequency of machine fit problems has not diminished in the last few decades. Experiments were conducted on a fretting wear testing machine of amplitude range 10–200 μm, frequency range 4–120 Hz and surface roughness were recorded for both polished and unpolished condition. The correlation was made between changing parameters and variation in surface roughness. Friction fatigue is an important but almost unknown factor when load-bearing components are damaged at very low loads. Therefore, we will conduct an experimental study of fretting and its control parameters. For unpolished specimen, the variation of amplitude with respect to the coefficient of friction (COF) increases to 0.5, then it becomes linear. For semi-polished specimen, it increases to COF 0.45 and then it starts decreasing. For a fully polished specimen, there is no change in COF to 75 μm and then it starts increasing. According to the experimental data, for all specimens' COF constantly decrease with increasing the load.

**Keywords**: Fretting wear, Coefficient of friction, Amplitude and vibration

## 1 Introduction

In most cases, the entirety of people makes wear out because of the relative motion among the surfaces. According to gadget failure analysis, in maximum cases, screw-ups of interacting shifting elements consisting of gears, bearings, clutches, cams, and clutches are laid low with lubrication and put on. Despite our certain understanding of many areas, the lubrication of human joints is not understood. Tribology has a much extra effect on our lives than is normally expected. For example, lengthy earlier than aware management of friction and put on became promoted, people and animals instinctively modified friction and put-on as they affected their bodies. It is a famous truth that human pores and skin sweats are in reaction to strain and anxiety. It became lately located that sweating on the arms or soles of people and dogs, instead of rabbits, can grow friction between the arms or paws and the strong floor [1]. In different words, whilst an animal or human feels dangerous, it sweats, facilitating a brief break out from the damaging area, or the capacity to keep a weapon or climb the closest tree. Non-mechanical slip structures offer many examples of this movie formation. Investigation of motion among adjoining geological plates at the floor has proven, for example, that rock crushing and a skinny layer of water shape among opposing rocks. The chemical response between rock and water is thought to be due to unusual place excessive temperatures (approximately 600 ºC)

and pressure (approximately one hundred MPa) [1], which improves the lubrication characteristic of the fabric on this layer. Laboratory checks of the fault version have proven that the slip starts have evolved to shape a self-slip layer of fragmented rock on the interface with tough rock. A pair of self-sealing layers connected to each rock save you water leaks wished for the lubrication impact of the rock and internal water layers [2]. The thickness of the intermediate layers of beaten rock is assumed to be 1–100 m. However, this thickness is not enormous in comparison to the variety of geological plates and those layers may be labeled as movies. Therefore, slippage at the geological scale is managed with the aid of using the houses of those lubricating membranes, whether or not on a massive geological scale or a microscopic scale of slippage among crimson blood cells and capillaries. It indicates a fundamental similarity among morphological slips. The formation and sturdiness of such movies are because of the truth that skinny movies are robotically stable. It may be very hard to pinch the sort of movie among items and expel it completely [3]. It is now no longer hard to squeeze out a part of the movie, but it is in reality not possible to remove it.

Abrasive wear occurs when a hard rough surface slides across a softer surface. ASTM International defines it as the loss of material due to hard particles or hard protuberances that are forced against and move along a solid surface.

### 1.1 *Abrasive wear*

Abrasive wear is commonly classified according to the type of contact and the contact environment. The type of contact determines the mode of abrasive wear. The two modes of abrasive wear are known as two-body and three-body abrasive wear. Two-body wear occurs when the grits or hard particles remove material from the opposite surface. Three-body wear occurs when the particles are not constrained and are free to roll and slide down a surface. The contact environment determines whether the wear is classified as open or closed. An open contact environment occurs when the surfaces are sufficiently displaced to be independent of one another [4], [5].

### 1.2 *Corrosive wear*

This kind of wear occurs in a variety of situations both in lubricated and un-lubricated contacts. The fundamental cause of these forms of wear is a chemical reaction between the worn material and the corroding medium. This kind of wear is a mixture of corrosion, wear and the synergistic term of corrosion-wear which is also called tribo-corrosion.

**Figure 1**: Fretting wear on the inside of bearings.

### 1.3 *Fretting wear*

Scuffing happens while a quick amplitude that slides to and fro among touch surfaces is maintained over some cycles. Over time, rubbing eliminates fabric from one or each of the surfaces in touch. The floor of maximum bearings is hardened to face up to the trouble; however, this typically takes place with bearings. A crack in one of the surfaces (shown in Figure 1), referred to as fretting fatigue, creates other trouble. It is the greater critical of the 2 phenomena as it is able to result in bearing failure. Associated trouble arises when small debris is eliminated via way of means of put on are oxidized withinside the air [6]. Oxides are typically more difficult than the underlying metallic, so if difficult debris keeps to put on the metallic floor, put on will accelerate. Fretting corrosion works the same, specifically within side the presence of water. Unprotected bearings on big systems along with bridges can extensively lessen performance, specifically when salt is used to de-ice highways supported via way of means of bridges in winter. The fretting trouble changed into associated with the Silver bridge tragedy and the Minus River bridge accident.

Scuffing takes place while a quick amplitude that slides from side to side among touch surfaces is maintained over some cycles. It results in varieties of harm: floor put on and decreased fatigue life (Figure 2). The diploma of damage and floor harm is a whole lot extra than the dimensions of the slide distance suggests. A small reciprocating movement with an

**Figure 2**: Fretting of threads in bolts.

amplitude of 0.1 μm can result in element failure if the slide lasts extra than 1 million cycles. Contacts that seem to have not any relative motion, which includes press suit, can slide inside a variety of 1 μm with alternating pendulum masses. It could be very hard to do away with such actions and the ensuing friction. Fretting put on and frictional fatigue arises on nearly each device and in any other case purpose a complete failure of strong additives. Studies have proven that in the evaluation of different kinds of put on, the frequency of device suit troubles has now no longer dwindled in current decades. Friction fatigue stays vital however in large part unknown issue inside the failure of load-bearing additives below very low masses [7], [8]. Therefore, the expertise of fretting is most usually crucial for engineers or technicians who address the reliability of equipment with a massive variety of low-amplitude slide contacts.

The primary feature of fretting is the very small slide amplitude that determines the inherent traits of this put on mechanism. Under positive situations of everyday and tangential masses at the contacts, microscopic motion takes place in the contacts, even within side the absence of hard slides. The middle of touch stays desk bound and the rims reciprocate with amplitudes at the order of one micron, inflicting fretting harm. Therefore, from a realistic factor of view, there is no decrease in restriction to the tangential pressure required for frictional harm, which needs to be taken into consideration while designing mechanical parts. One of the hallmarks of fretting is its low amplitude, which regularly leaves the generated put on in touch [9], [10]. Accumulated put on regularly separates each surface and, in a few cases, can make contributions to accelerating the wear and tear procedure. The fretting procedure may be additionally increased with the aid of using corrosion, temperature, and different effects. Microscopic motion inside contacts below implemented load When solids are compressed after which subjected to a tangential pressure that will increase in magnitude, a macroscopic slide takes place at a specific tangential pressure value. This is a famous experimental fact; however, it is not always widely known that tangential pressure stages under this restrict additionally purpose tangential tremors in reaction to implemented forces. These micro motions were observed to be an essential belongings of Hertz touch uncovered to tangential forces [11], [12]. There are fashions that describe the conduct of such contacts. The former "elastic" version and the lately developed "elasto-plastic" version.

## 2 Materials and Methodology

### 2.1 *Material composition and properties*

Flats are prepared from SS316L material (composition in Table 1). The amplitude of movement at any point in the contact area may be nominally the same as in the coarse glide state (properties listed in Table 2).

**Table 1**: Workpiece composition

| Element | SS316L |
|---|---|
| Fe | 67.12 |
| Cr | 17.15 |
| Ni | 10.23 |
| Mo | 2.04 |
| Mn | 1.75 |
| C | 0.029 |
| Co | 0.1 |
| Cu | 0.36 |
| Nb | 0.04 |
| V | 0.05 |
| W | 0.05 |
| Si | 0.44 |
| P | 0.043 |
| S | 0.03 |
| Al | 0.01 |
| Ti | 0.01 |

**Table 2**: Mechanical properties of SS-316L

| Material | Young's Modulus (GPa) | Vicker Hardness |
|---|---|---|
| SS316L | 210 | 284 |

### 2.2 *Elastic model for fretting contacts*

Normal stress $p$ in a stationary Hertzian contact rises smoothly from zero at the edge of the contact to its maximum value at the center of the contact. Assuming that the coefficient of static friction $\mu$ across the contact is constant, the frictional stress μp, resulting from the normal stress $p$, also rises smoothly from zero at the edge of the contact to a maximum value at the center [13]. If an external tangential force $Q < \mu W$ is subsequently applied to the contact and no slip occurs, then the resulting tangential stress $q$ rises from some finite value at the middle of the contact to an infinite value at the edges as shown in Figure 3. The distribution of tangential stress q can be calculated using Equation (1) across, e.g., a circular contact, which can be described by the following expression [14]:

$$q_x = Q / 2\pi a(a^2 - x^2)0.5 \quad (1)$$

Where $q_x$ is the calculated tangential stress along the $x$ axis (Pa).

$a$ is the radius of the contact area (m).

$Q$ is the superimposed tangential force (N).

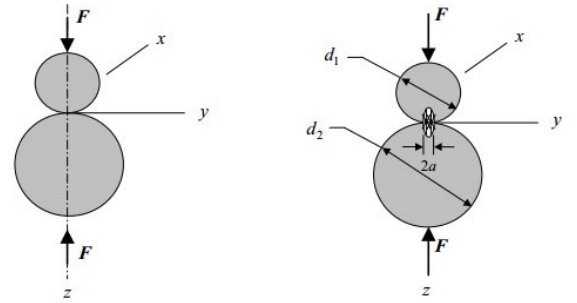


(a) Two spheres held in contact by force $F$.

(b) Contact stress has an elliptical distribution across contact over zone of diameter $2a$.

**Figure 3**: Two spheres in contact.

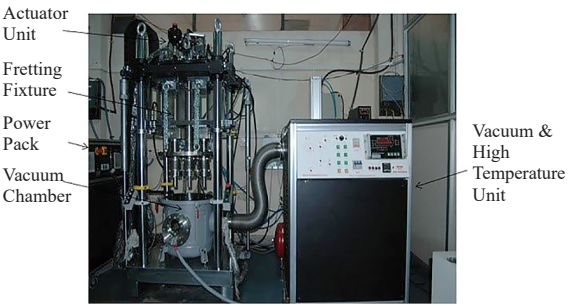


**Figure 4**: Fretting wear machine.

### 2.3 *Methodology*

The main requirement in building a friction test for a stand is the ability to generate tangential vibrational relative motion of only 1 μm between two contact surfaces [15]. The amplitude of movement at any point in the contact area may be nominally the same as in the coarse glide state (properties listed in Table 2), or it may vary from point to point in the partial glide state. To maintain a given deflection amplitude under a constant vertical load, the tangential force applied is sufficient to handle the increase in friction coefficient or shear force that can occur as a result of adhesion between the contact surfaces must be large (That machine setting and arrangement is shown in Figures 3 and 4). Fretting damage studies are generally performed by applying either known tangential forces or known tangential displacements. When a known tangential force is applied, the contact adapts by reacting in the form of a tangential force. In force control experiments, reduced friction between contact surfaces can lead to a transition from partial slip to coarse slip. Therefore, in force control tests, changes in the state of the interface can dramatically change the state of strain at the interface. Displacement control tests are recommended if you want to investigate the effects of strain conditions. Force control tests are stable only if they function under partial slip conditions, but displacement control tests do not raise stability issues. In this way, crack formation and wear can be better investigated under displacement-controlled conditions [16], [17].

### 2.4 *Hertzian contact analysis*

*Characteristics of Contact Stresses*

1) Represent compressive stresses developed from surface pressures between two curved bodies pressed together.

2) Possess an area of contact. The initial point contact (spheres) or line contact (cylinders) become area contacts, as a result of the force pressing the bodies against each other.

3) Constitute the principal stresses of a tri-axial

(three-dimensional) state of stress.

4) Cause the development of a critical section below the surface of the body.

5) Failure typically results in flaking or pitting on the body's surfaces.

Consider two solid elastic spheres held in contact by a force $F$ such that their point of contact expands into a circular area of radius a, given in Equation (2).

$$a = K_a \sqrt[3]{F} \tag{2}$$

Where

$$K_a = \left[\frac{3}{8}\frac{(1-V_1^2)/E_{1+}(1-V_2^2)/E_2}{(1/d_1)+(1/d_2)}\right]^{\frac{1}{3}} \tag{3}$$

$F$ = applied force
$V_1$, $V_2$ = Poisson's Ratio for spheres 1 and 2
$E_1$, $E_2$ = Elastic Moduli for spheres 1 and 2
$d_1$, $d_2$ = diameter of spheres 1 and 2

Equation (3) used for the contact radius can be applied to case the Sphere in contact with a plane ($d_2 = \infty$).

The maximum contact pressure, $p_{max}$, occurs at the center point of the contact area.

$$p_{\max} = \frac{3F}{2\pi a^2}$$

### 2.5 *Calculation of principal stresses*

$$\sigma_x = -p_{max}\left[\left[1-|\zeta_a|\tan^{-1}\left(\frac{1}{|\zeta_a|}\right)\right](1+V)-\frac{1}{2\left(1+\zeta_a^{\,2}\right)}\right]$$

$$= \sigma_y = \sigma_1 = \sigma_2$$

$$\sigma_3 = \sigma_z = \frac{-p_{max}}{1+\zeta_a^{\,2}}$$

Where $\zeta_a$ = z/a = nondimensional depth below the surface

$V$ = Poisson's ratio for the sphere examined (1 or 2)

### 2.6 *Workpiece surface roughness*

Flats are prepared from SS316L material (composition in Table 1). The dimensions of the sample are 80 × 15 × 10. These flats are polished using emery sheets to obtain the desired surface roughness Initial polishing is done using the emery sheets with the number designated as 120 and then this is increased till 2000 (shown in Figure 5). In this experiment, there are three variables factors are considered for the test which are load, amplitude and surface polish (Tables 3 and 4).

**Table 3**: Hertzian analysis applied at the point of contact: 3 mm ball diameter

| Sl.No | Normal Load (N) | Area of contact, $a$ (mm) | Maximum Pressure, $p_{max}$ (N/mm$^2$) | Tri-axial Stresses (N/mm$^2$) | |
|---|---|---|---|---|---|
| | | | | $\sigma_x = \sigma_y$ | $\sigma_z$ |
| 1 | 200 | .1263 | 5986.38 | –1938.389 | –5491.905 |
| 2 | 300 | .1445 | 6860.04 | –2221.282 | –6293.40 |
| 3 | 400 | .1591 | 7545.03 | –2443.080 | –6921.810 |
| 4 | 500 | .1714 | 8126.24 | –2631.277 | –1455.014 |
| 5 | 600 | .1821 | 8369.184 | –2797.367 | –7925.587 |

**Table 4**: Hertzian analysis applied at the point of contact: 6.35 mm ball diameter

| Sl.No | Normal Load (N) | Area of contact, $a$ (mm) | Maximum Pressure, $p_{max}$ (N/mm$^2$) | Tri-axial Stresses (N/mm$^2$) | |
|---|---|---|---|---|---|
| | | | | $\sigma_x = \sigma_y$ | $\sigma_z$ |
| 1 | 200 | .1625 | 3616.30 | –1170.957 | –3317.593 |
| 2 | 300 | .1861 | 4135.898 | –1339.203 | –3794.278 |
| 3 | 400 | .2048 | 4553.459 | –1474.410 | –4177.340 |
| 4 | 500 | .2206 | 4905.693 | –1588.463 | –4500.482 |
| 5 | 600 | .2344 | 5214.076 | –1688.317 | –4783.393 |

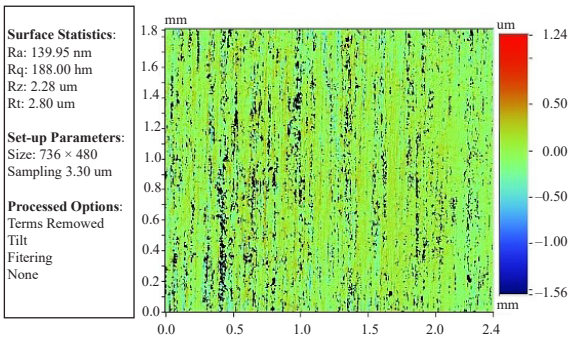


**Figure 5**: The images obtained by the optical profilometer. The images are obtained at magnification 2.5X in VSI mode.

## 3 Experiment Result and Discussion

### 3.1 *Experiment #1*

| Parameters | Specification |
|---|---|
| Amplitude | 25 µm |
| Frequency | 5 Hz |
| Number of Cycles | 900 |
| Load | 200 N |

Table 4 shows experimental data to conduct the experiment. A graph is plotted with numbers of cycles on x-axis and tangential load on y-axis shown in Figures 6 and 7. It is evident that a complete transition from slip regime to stick regime takes place at a faster rate with the various regimes overlapping each other. A graph is plotted with numbers of cycles on x-axis and coefficient of friction on y axis. It is evident that after the initial running in period and transition stage, the coefficient of friction reaches a steady value.

### 3.2 *Experiment #2*

| Parameters | Specification |
|---|---|
| Amplitude | 50 µm |
| Frequency | 5 Hz |
| Number of Cycles | 900 |
| Load | 200 N |

A graph is plotted with numbers of cycles on x-axis and tangential load on y-axis shown in Figures 8 and 9. It is evident that the complete transition from slip regime to stick regime takes place gradually such that the various stages of transition can easily be distinguished.

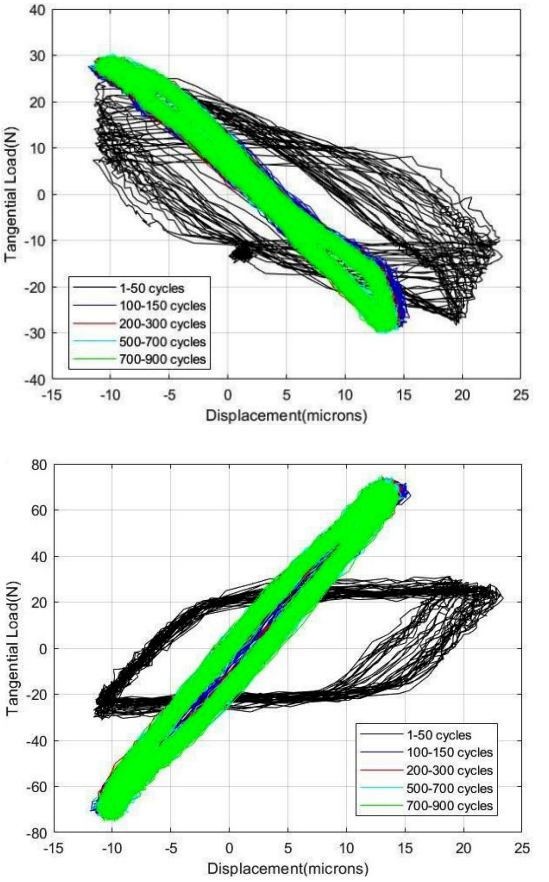


**Figure 6**: Surface roughness unpolished graph plotted with numbers of cycles.

A graph is plotted with numbers of cycles on x-axis and coefficient of friction on y axis. It is evident that coefficient of friction does not reach a steady value and continues to vary.

### 3.3 *Experiment #3*

| Parameters | Specification |
|---|---|
| Amplitude | 75 µm |
| Frequency | 5 Hz |
| Number of Cycles | 900 |
| Load | 200 N |

A graph is plotted with numbers of cycles on x-axis and tangential load on y-axis shown in Figures 10 and 11. It is evident that a complete transition from slip regime to stick regime does not take place. It continues the transition in the stick slip regime.

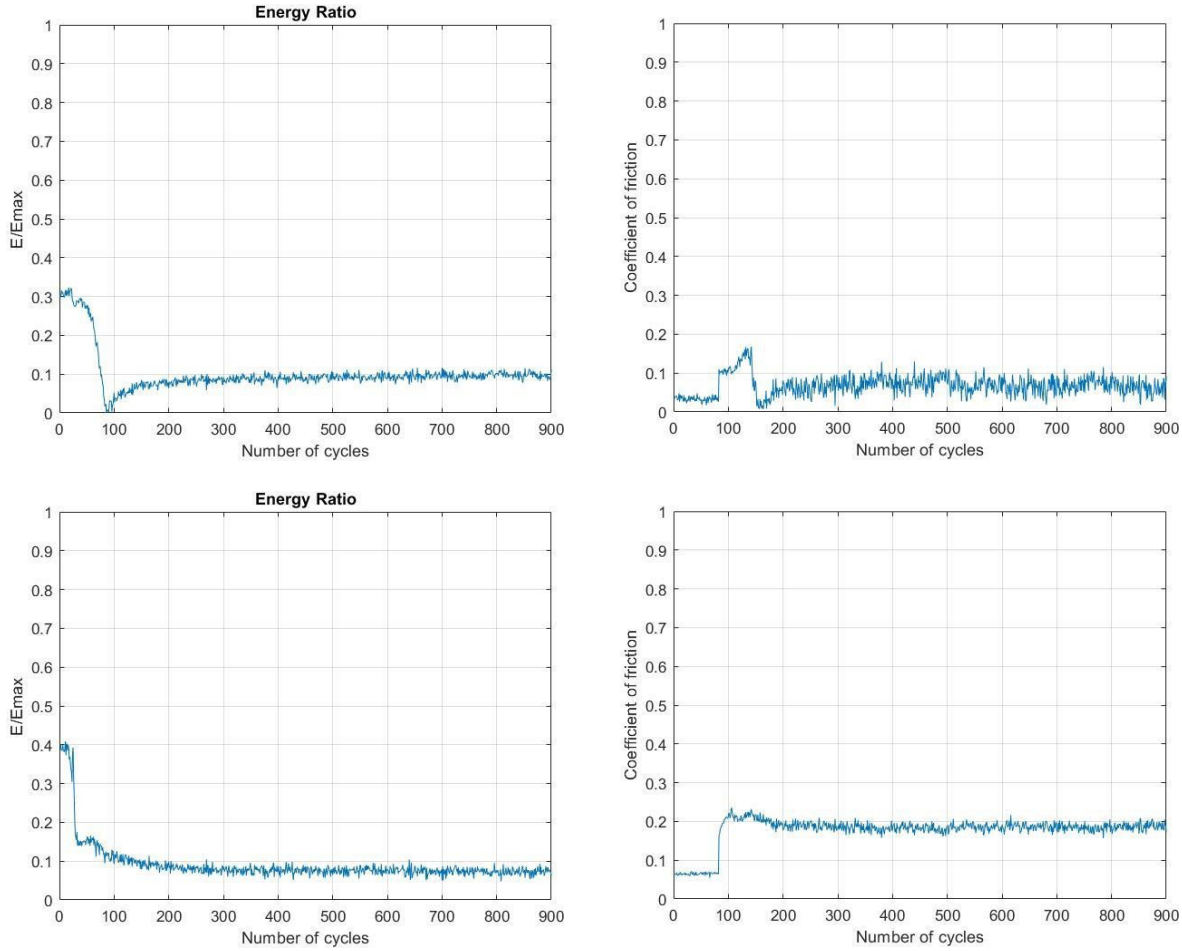


**Figure 7**: Graphs plotted with numbers of cycles on x-axis and tangential load on y-axis.

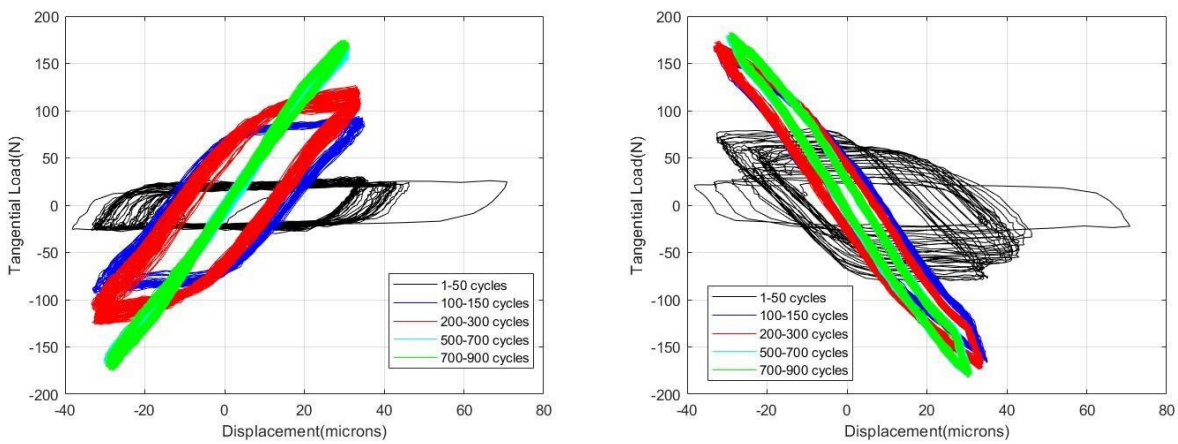


**Figure 8**: Surface roughness unpolished graph plotted with numbers of cycles.

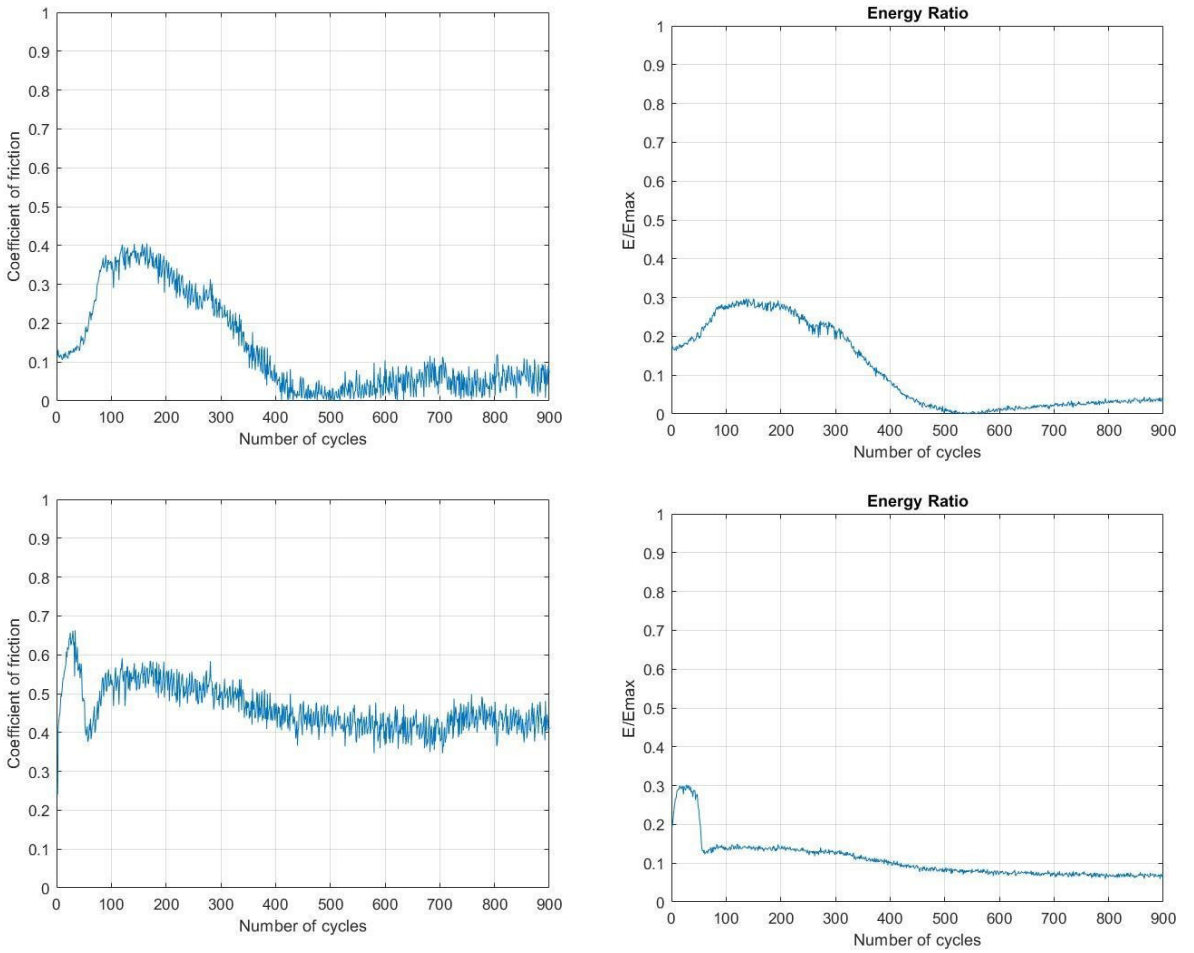


**Figure 9**: Graphs plotted with numbers of cycles on x-axis and tangential load on y-axis.

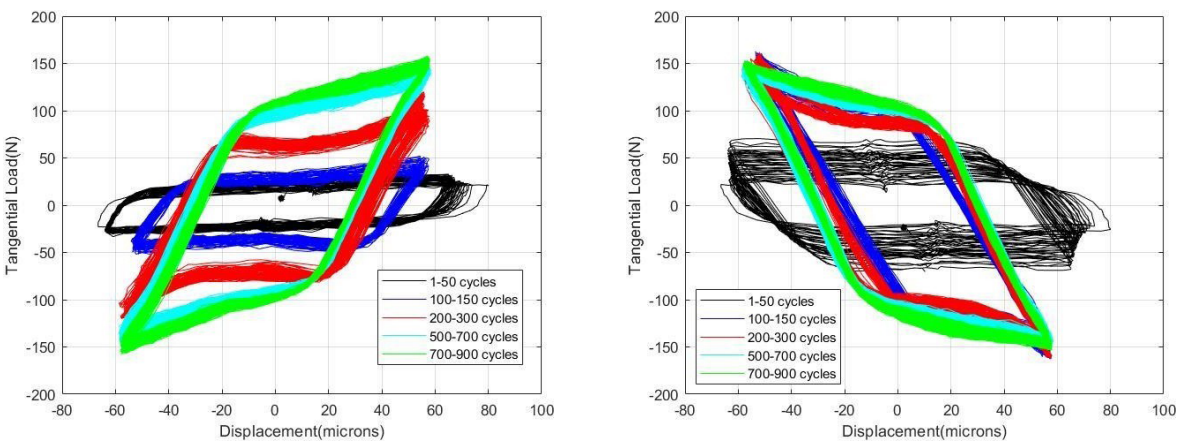


**Figure 10**: Surface roughness unpolished graph plotted with numbers of cycles.

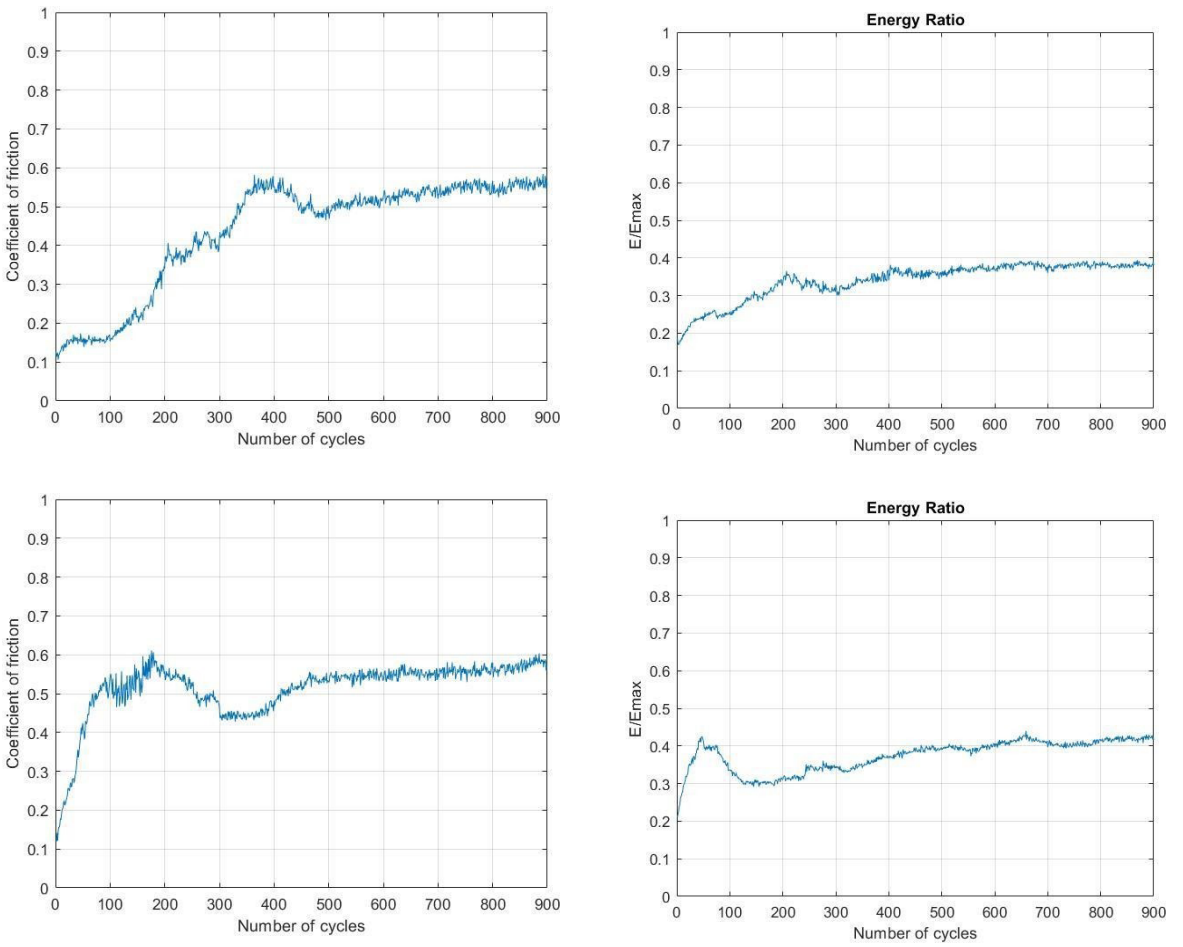


**Figure 11**: Graphs plotted with numbers of cycles on x-axis and tangential load on y-axis.

A graph is plotted with numbers of cycles on x-axis and coefficient of friction on y axis. It is evident that coefficient of friction does not reach a steady value and continues to vary with steady increase in value.

### 3.4 *Experiment #4*

| Parameters | Specification |
|---|---|
| Amplitude | 100 μm |
| Frequency | 5 Hz |
| Number of Cycles | 900 |
| Load | 200 N |

A graph is plotted with numbers of cycles on x-axis and tangential load on y-axis shown in Figures 12 and 13. It is evident that a complete transition from slip regime to stick regime does not take place. It continues the transition in the stick slip regime with higher amplitudes not reaching a steady state.

A graph is plotted with numbers of cycles on x-axis and coefficient of friction on y axis. It is evident that after the initial running in period and transition stage, the coefficient of friction reaches a steady value.

The following inferences have been made after concluding the above list of experiments.

*Variable normal load:*

Irrespective of the ball diameter the coefficient of friction decreases with an increase in load this is true for both polished and unpolished surfaces [18], [19]. For both ball diameters, the number of cycles required to achieve stick regime decrease with increase in load

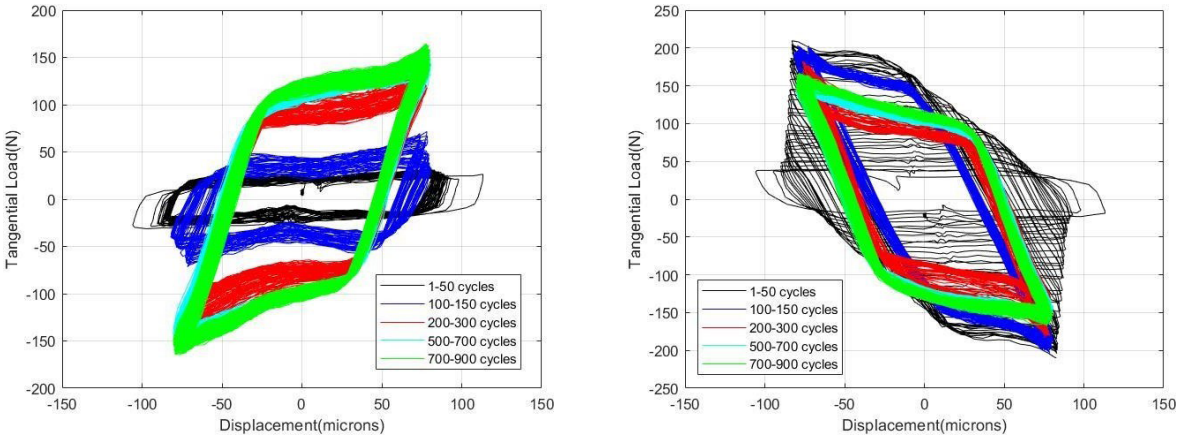


**Figure 12**: Surface roughness graph plotted with numbers of cycles.

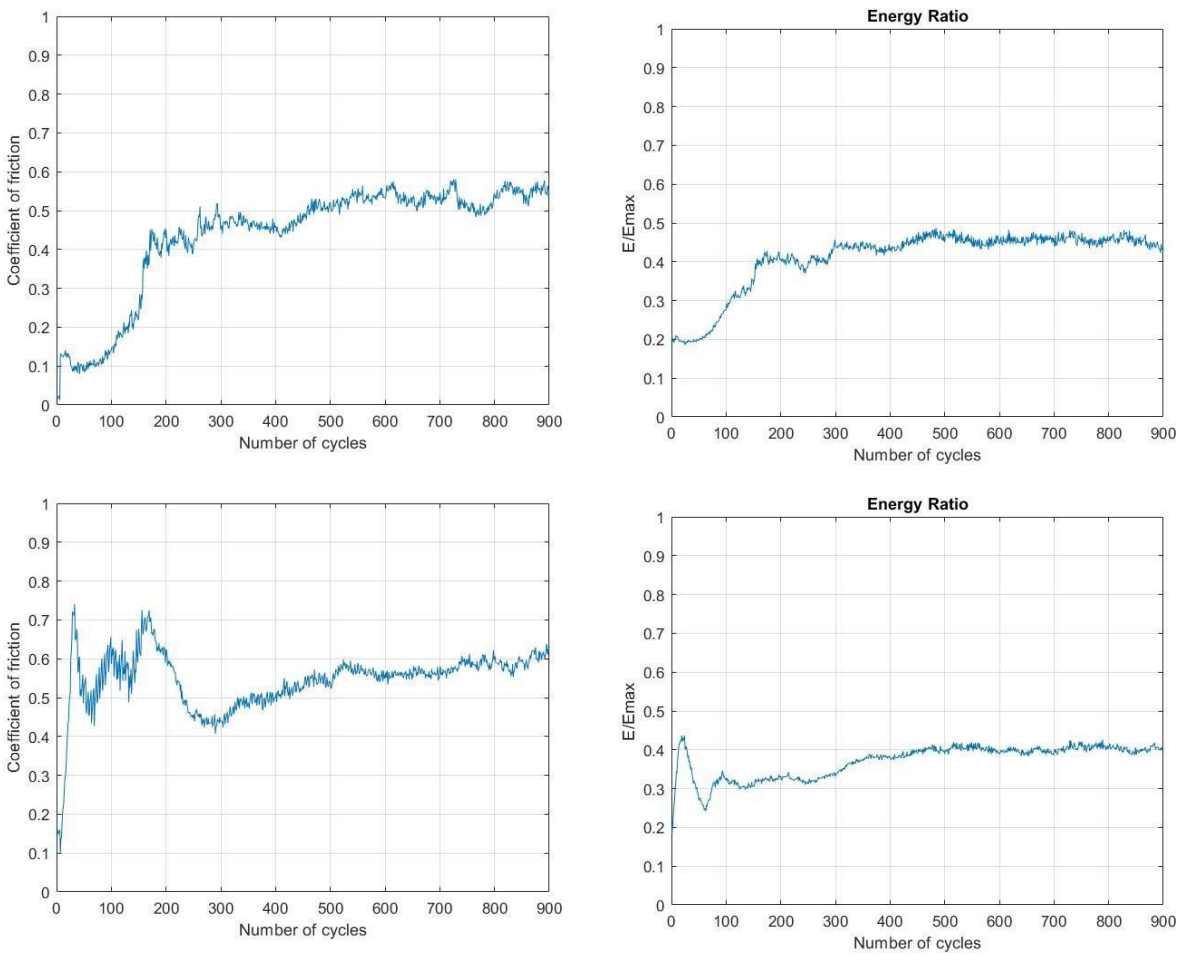


**Figure 13**: Graphs plotted with fixed numbers of cycles.

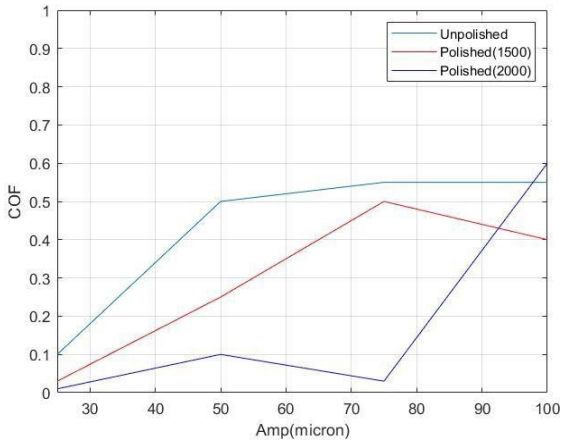


**Figure 14**: 3 mm ball amplitude variation.

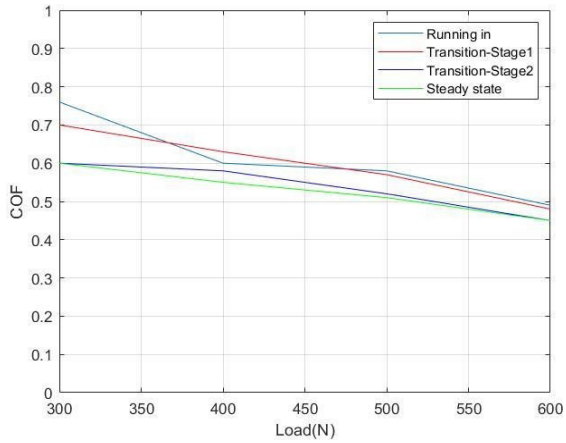


**Figure 15**: 6.35mm ball: Load variation (polished: 2000).

as shown in Figures 14 and 15. For polished sample and small ball diameter, the difference between the running in and steady-state coefficient of friction values are the same for all loads. Whereas, for bigger diameter ball, this difference between the running in and steady state is decreasing.

The variation in coefficient friction during the transition stage decreases with an increase in load [20], [21] and this is more prominently visible with larger diameter ball as compared with smaller diameter ball for both polished and unpolished surfaces.

*Variable amplitude:*

In all the experiments the general trend is that the coefficient of friction is increasing with increasing amplitude for both diameters and surfaces. With increasing amplitude, the steady state reached changes from stick regime to slip-stick regime for both the diameters and surfaces. For a bigger ball diameter, the coefficient of friction for a smaller amplitude is lower than that of a smaller ball diameter, but in case of a higher amplitude, this trend is nonuniform. For unpolished surface, the variation of coefficient of friction with amplitude for both bigger and smaller balls is nearly the same but in case of polished surface, this variation is non-linear.

*Variable surface roughness:*

Coefficient of friction for unpolished surfaces are having higher values as compared to polished surfaces for both balls. For unpolished surface, the variation of coefficient of friction in ball diameter ball is less compared to the bigger diameter ball. This is due to higher contact pressure in a small ball and the flat contact, which causes the flattening of the asperities during the load application itself. The effect of surface roughness is more predominantly seen while varying the amplitude, with the coefficient of friction varying continuously as in case of unpolished surface compared to polished surface where it might reach a steady value. In case if varying load, the effect of surface roughness is observed only in case of lower loads for unpolished surface. Whereas this is not observed for polished surface.

*Variable Ball Diameter:*

The coefficient of friction is higher for a bigger ball diameter compared to a smaller ball diameter for increasing normal load. While the coefficient of friction is higher for smaller diameter ball compared to bigger diameter ball for increasing amplitude. Both bigger and smaller diameter balls have the similar coefficient of friction variation for unpolished surface under varying amplitude. Whereas this variation is non-uniform in case of polished surface. The difference in the value of the coefficient of friction between the running in and the steady state is larger for the bigger diameter ball as compared to the smaller diameter ball for both polished and unpolished surfaces.

## 4 Conclusions

These experiments advantage perception into fretting put on and additionally take a look at an impact it

could have on fabric put on and particle formation. Microscope exams of fretted surfaces and fretting particles yielded enough records to assemble an in-depth description of the fretting of metallic within side the air. It turned into determined that the steel fretting particles turned shaped through the split of the fretted floor into small steel flakes. The flake morphology supported a mechanism of formation based totally on the delamination principle of put on. Abrasive put-on or metallic switch through adhesion did now no longer provide an explanation for the morphology and consequently had been dominated out within side the gift case. The formation of the oxide particles in fretting might also arise through the oxidation of the fretting floor accompanied by the scraping away of this floor oxide or through the oxidation of steel put on particles. Experimental observations and theoretical evaluation confirmed that the touch situations in fretting alternate with growing displacement amplitude. Three specific regimes of fretting are outstanding in the usage of dynamic tangential pressure and displacement measurement.

**Author Contributions**

J.R.: conceptualization, investigation, reviewing; N.H.L.: investigation, methodology, writing an original draft editing and formatting; D.S.: data analysis, corrections graphs and formatting; All authors have read and agreed to the published version of the manuscript.

**Conflicts of Interest**

The authors declare no conflict of interest

**Reference**

[1] T. Yue and M. A. Wahab, "A review on fretting wear mechanisms, models and numerical analyses," *Computers, Materials & Continua*, vol. 59, no. 2, pp. 405–432, 2019, doi: 10.32604/cmc.2019.04253.

[2] I. R. McColl, J. Ding, and S. B. Leen, "Finite element simulation and experimental validation of fretting wear," *Wear*, vol. 256, no. 11–12, pp. 1114–1127, 2004, doi: 10.1016/j.wear.2003.07.001.

[3] R. B. Waterhouse, *Fretting Fatigue*. London: Applied Science, 1981.

[4] R. B. Waterhouse, *Fretting Wear*. Ohio: ASM International, 1992, pp. 233–256.

[5] Z. R. Zhou and L. Vincent, "Cracking induced by fretting of aluminium alloys," *Journal of Tribology*, vol. 119, no. 1, pp. 36–42, 1997, doi: 10.1115/1.2832477.

[6] M. H. Zhu, Z. R. Zhou, P. Kapsa, and L. Vincent, "An experimental investigation on composite fretting mode," *Tribology International*, vol. 34, no. 11, pp. 733–738, 2001.

[7] M. H. Zhu and Z. R. Zhou, "An experimental study on radial fretting behaviour," *Tribology International*, vol. 34, no. 5, pp. 321–326, 2001.

[8] Z. Cai, M. Zhu, and Z. Zhou. "An experimental study torsional fretting behaviors of LZ50 steel," *Tribology International*, vol. 43, no. 1–2, pp. 361–369, 2010.

[9] J. L. Mo, M. H. Zhu, J. F. Zheng, J. Luo, and Z. R. Zhou, "Study on rotational fretting wear of 7075 aluminum alloy," *Tribology International*, vol. 43, no. 5–6, pp. 912–917, 2010.

[10] Z. R. Zhou and L. Vincent, "Effect of external loading on wear maps of aluminium alloys," *Wear*, vol. 162, pp. 619–623, 1993.

[11] Z. R. Zhou and L. Vincent, "Mixed fretting regime" *Wear*, vol. 181–183, pp. 531–536, 1995.

[12] Z.R. Zhou, S. Fayeulle, and L. Vincent "Cracking behaviour of various aluminium alloys during fretting wear," *Wear*, vol. 155, pp. 317–330, 1992.

[13] M. H. Zhu and Z. R. Zhou, "On the mechanisms of various fretting wear modes," *Tribology International*, vol. 44, no. 11, pp. 1378–1388, 2011.

[14] J. F. Zheng, J. Luo, J. L. Mo, J. F. Peng, X. S. Jin, and M. H. Zhu, "Fretting wear behaviors of a railway axle steel," *Tribology International*, vol. 43, no. 5–6, pp. 906–911, 2010.

[15] R. D. Mindlin, "Compliance of elastic bodies in contact," *Journal of Applied Mechanics*, vol. 16, no. 3, pp. 259–268, 1949.

[16] O. Vingsbo and S. Söderberg, "On fretting maps," *Wear*, vol. 126, no. 2, pp. 131–147, 1988.

[17] P. Kapsa and L. Vincent, "Progress in fretting maps" *Tribology International*, vol. 39, no. 10, pp. 1068–1073, 2006

[18] M. H. Zhu, H. Y. Yu, Z. B. Cai, and Z. R. Zhou "Radial fretting behaviors of dental feldspathic ceramics against different counter bodies," *Wear*, vol. 259, no. 7–12, pp. 996–1004, 2005

[19] M. H. Zhu, H. Y. Yu, and Z. R. Zhou "Radial fretting behaviors of dental ceramics," *Tribology International*, vol. 39, no. 10, pp. 1255–1261, 2006.

[20] K. L. Johnson, *Contact Mechanics*. Great Britain, UK: Cambridge University Press, 1985.

[21] Z. B. Cai, M. H. Zhu, J. F. Zheng, X. S. Jin, and Z. R. Zhou, "Torsional fretting behaviors of LZ50 steel in air and nitrogen" *International Tribology*, vol. 42, no. 11–12, pp. 1676–1683, 2009.